New orbital solution for LS 5039 and search for period variability

Author: Gunnar Gutiérrez Lütken.
*Facultat de Física, Universitat de Barcelona, Diagonal 645, 08028 Barcelona, Spain.**

Advisor: Marc Ribó Gomis

Abstract: In recent decades, the study of high-energy gamma-ray emitting astrophysical objects has led to the discovery of a new type of object called gamma-ray emitting binaries (GREB). Among the approximately 30 known GREBs, several consist of a compact object and a massive star. The ones characterised by having the peak of their spectral energy distribution at $\gtrsim 1$ MeV are called gamma-ray binaries (γBs). So far, ten γBs, including LS 5039, have been confirmed as sources of high and/or very high-energy γ-ray emission. Understanding the physical processes of binary systems like LS 5039 is crucial. As their behaviour depends on the orbital phase, obtaining comprehensive information about the orbital parameters and their potential evolution is of great importance. In this work, we report the study of the evolution of the orbital period of LS 5039 through the fitting of orbital solutions to radial velocities using the program Spectroscopy Binary Orbit Program (SBOP). Our study revealed no significant variation within the observed time frame. The new orbital solution we derived, $P_{\rm orb} = 3.90599 \pm 0.00002$ day, is an order of magnitude more precise than the previous solution. Additionally, we assessed the potential impact of energy loss due to the emission of gravitational waves on the orbital period evolution, concluding that it was too small to significantly influence the results.

I. INTRODUCTION

During the last decades it has been possible to study high-energy gamma-ray emitting astrophysical objects only due to the development and optimisation of observatories and space-borne satellites at high-energies (HE, 100 MeV $< E <$ 100 GeV) and very-high-energies (VHE, $E >$ 100 GeV (Hinton & Hofmann, 2009). This enabled the discovery of binary systems emitting HE and/or VHE, and the emergence of a new type of object, the gamma-ray binaries (Dubus 2013).

There are about 30 gamma-ray emitting binaries (GREB) currently known. Among them, several binaries are composed of a compact object and a massive star. The ones that are powered by accretion from the companion star onto the compact object, which can be either a neutron star or a stellar-mass black hole, are called *microquasars*, like Cyg X-3 or Cyg X-1 . Binary objects distinguished for having the peak of their spectral energy distribution (SED) at $\gtrsim 1$ MeV are named *gamma-ray binaries* (γBs, Bordas 2023).

Ten gamma-ray binaries, including LS 5039, have been so far confirmed as sources of HE and/or VHE γ-ray emission. Three of them have been confirmed as radio pulsars: PSR B1259−63, PSR J2032+4127, LS I +61 303. Evidences indicate that these sources are young non-accreting neutron stars. In the other cases the nature of the compact object is unknown. It is widely accepted that, even if no pulsations have been detected, the phenomenological similitudes between the sources strongly indicate a pulsar-powered scenario in most of them (Dubus 2013, Paredes et al. 2019, Bordas 2023).

Theoretically, the emission from γBs is produced at the interface of the pulsar wind and the stellar wind from the massive companion star, where particle acceleration can reach high-efficiency levels. The inverse Compton (IC) scattering of relativistic electrons and positrons off seed photons that are provided by the companion star (or photons produced in the circumstellar disk, if there is one), is what generates the γ-rays (see Dubus 2013 and references therein).

LS 5039 was identified as a VHE source in 2005, firstly as high-mass X-ray binary, from a cross-correlation of unidentified ROSAT X-ray sources with OB star catalogues. Paredes et al. (2000) noted that LS 5039 was within the 0.5° error box of the EGRET source 3EG 1824−1314, suggesting it as a possible γ-ray source.

In order to model and understand the physical processes of a binary system as LS 5039, as its behaviour is dependent on its orbital phase, it is of strong importance to know and obtain all the possible information about the orbital parameters. In this work, we report the study, through the fitting of orbital solutions to radial velocities, of the evolution of the orbital period of LS 5039 to see if there is any variation (hints have been found at high energies, J. Casares private communication). In Sect. II we report the observational data and the studies conducted to obtain the radial velocities. In Sect. III the method used to fit the data in order to obtain the orbital parameters is described. In Sect. IV we discuss the analysis carried out to determine the orbital parameters and their evolution, as well as the obtained results. Motivated by recent advances in gravitational wave research and future opportunities they provide, in Sect. V we conduct a study to assess how the energy loss through the emission of gravitational waves could impact on the evolution of the orbital period. Finally, the conclusions of this work are presented in Sect. VI.

*Electronic address: ggutielu7@alumnes.ub.edu

TABLE I: Summary of the data used in this work

Epoch	Telescope / Observatory	Number of points	Reference
1998–03	0.9 m CFT KPNO	54	McSwain et al. (2001, 2004)
2002–03	2.5 m INT ORM	197	Casares et al. (2005)
2005	1.9 m RT SAAO	28	J. Casares (priv. comm.)
2007–09	2.5 m INT ORM	122	J. Casares (priv. comm.)
2007–08	1.5 m SMARTS CTIO	50	Aragona et al. (2009)
2010–11	2.0 m LT ORM	49	J. Casares (priv. comm.)
2018–22	2.5 m INT ORM	62	J. Casares (priv. comm.)

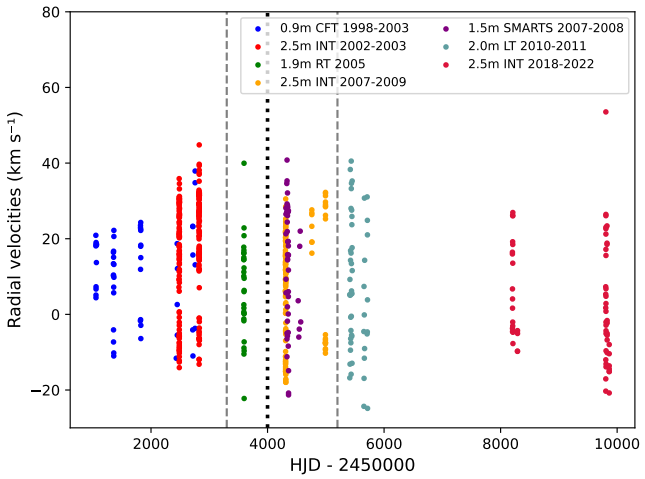

FIG. 1: Radial velocities as a function of time for the different data sets listed in Table I.

II. OBSERVATIONAL DATA

The dataset used in this study comprises observational data collected from multiple investigations conducted spanning the period from 1998 to 2022. Each investigation obtained specific radial velocity measurements within distinct time intervals. Comprehensive details regarding the corresponding epoch of observation periods, the telescopes and observatories involved in the data acquisition, the number of data points and the references are presented in Table I.

The data obtained from J. Casares through private communication, which were collected using the Isaac Newton Telescope (INT) at the Observatorio del Roque de Los Muchachos (ORM) and the 1.9 meters Radcliffe Telescope (RT) at the South African Astronomical Observatory (SAAO), were processed using the same methodology as detailed in the work by Casares et al. (2005). Similarly, the data acquired using the Liverpool Telescope (LT) from ORM were treated following the same procedures outlined in Casares et al. (2012). The data referenced in McSwain et al. (2001, 2004) were collected using the 0.9 m Coudé Feed Telescope (CFT) from the Kitt Peak National Observatory (KPNO), and the data referenced in Aragona et al. (2009) was taken with the 1.5 m SMARTS Telescope (SMARTS) from the Cerro Tololo Inter-American Observatory (CTIO).

We show in Fig. 1 the radial velocities as a function of time expressed in Heliocentric Julian Day minus 2450000 for better display (HJD−2450000). The analysis of this work primarily focused on two distinct divisions. The first division consisted of three blocks (separated by the dashed grey vertical lines in Fig. 1), namely 1998–2003, 2005–2009, and 2010–2022, comprising 251, 240, and 111 data points, respectively. The second division includes two blocks (separated by the dotted black vertical line in Fig. 1), 1998–2005 and 2007–2022, with 279 and 283 data points, respectively.

III. RADIAL VELOCITY FITTING WITH SBOP

The radial velocity fits that are described in the following sections were computed using the code Spectroscopy Binary Orbit Program (SBOP, P. Etzel 2004). This code allows the user to fit the radial velocity data to an eccentric orbit model for a single-line solution or a double-line solution. The following parameters can be fit: orbital period ($P_{\rm orb}$), epoch of periastron (T_0), argument of periastron (ω) eccentricity (e), systemic velocity (v_0) and velocity semi-amplitude (K).

The SBOP program is run by giving different values to the input parameters, and setting them as fixed or variable. If the program is able to find a solution where it fits the radial velocities with the given inputs, it returns the parameters of the fitted solution and 1σ uncertainties. We used slightly different input parameters and checked that the output parameters were always the same. Therefore, all the fits were accepted as valid.

When fitting radial velocities, SBOP also gives the orbital phases for the input radial velocities and the theoretical curve corresponding to the fitted solution.

IV. RESULTS AND DISCUSSION

The best orbital solution currently known for the orbital parameters of LS 5039 is found in Casares et al. (2005): $P_{\rm orb} = 3.90603 \pm 0.00017$ day, $e = 0.31 \pm 0.04$, $\omega = 226 \pm 8°$, $v_0 = 8.1 \pm 0.5$ km s^{-1} and $K = 19.4 \pm 0.9$ km s^{-1}. Due to new data being added to the existing records, we conducted a new analysis using SBOP to find

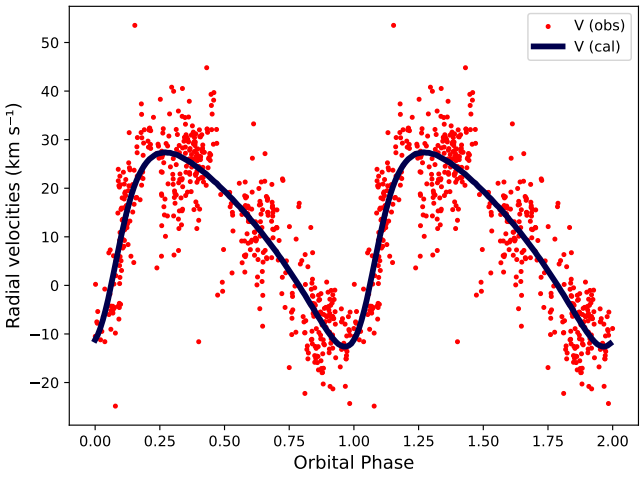

FIG. 2: Radial velocities plotted as a function of the orbital phase, and the optimal fit for the whole data set (1998–2022) setting all the parameters as variable. Two cycles are shown for better display.

the solution that best fitted the updated data set.

A. First analysis: all data points

The input parameters employed were sourced from Casares et al. (2005) and were all set as variable. The output parameters correspond to the new optimal orbital solution. SBOP returned an orbital period value of $P_{\rm orb} = 3.90599 \pm 0.00002$ day, which is an order of magnitude more precise than the previous orbital solution from Casares et al. (2005). The other parameters corresponding to this new orbital solution are: $e = 0.35 \pm 0.03$, $\omega = 243 \pm 5$ °, $v_0 = 10.5 \pm 0.3$ km s^{-1} and $K = 20.0 \pm 0.6$ km s^{-1}, which are similar but more precise than the ones previously known. We show in Fig. 2 the radial velocities of LS 5039 as a function of the orbital phase, and the fitted solution to all data points. The output orbital parameters of this fit were then used as the input parameters for SBOP in the following analyses (see Subsect. IV B and Subsect. IV C).

In Table II we show the epoch of the radial velocities used and the corresponding returned orbital parameters of all the analyses. A_1 corresponds to the analysis including all data points and the new orbital solution. The uncertainties are represented as the numbers in parentheses next to the values, and correspond to the uncertainties in the last quoted digit. The parameters without uncertainties were set as fixed for the corresponding analyses.

B. Second analysis. Three blocks

The next step in the study of the data set was to split it in different blocks, so that the evolution of the orbital parameters could be detected by comparing the results obtained from each block. For that, each block should include enough data for the results to be significant, and the epochs of observation included in each block should be as similar in length as possible. Following this guidelines, we ended up with the divisions discussed in Sect. II.

TABLE II: Orbital solutions for the parameters

Block	Epoch	$P_{\rm orb}$ (day)	T_0 (HJD−2450000)	e	w (°)
A_1	1998–2022	3.90599(2)	5400.11(4)	0.35(3)	243(5)
B_1	1998–2003	3.90599(2)	5400.11	0.35	243
B_2	2005–2009	3.90608(7)	5400.11	0.35	243
B_3	2010–2022	3.90595(5)	5400.11	0.35	243
C_1	1998–2005	3.90600(3)	5400.11	0.35	243
C_2	2007–2022	3.90597(4)	5400.11	0.35	243
C_3	1998–2005	3.90599(3)	5400.11	0.38(3)	243
C_4	2007–2022	3.90597(4)	5400.11	0.32(3)	243
C_5	1998–2005	3.90607(20)	5400.07(12)	0.39(3)	231(6)
C_6	2007–2022	3.90597(4)	5400.21(5)	0.35(3)	256(6)

Firstly, a three-block division was considered, in order to have three orbital solutions to be compared and to see if there was any evidence of a clear trend in the variation of the orbital period. Taking into account the distribution of the data set (as seen in Fig. 1), the set was divided in the three blocks B_1, B_2 and B_3 detailed in Table II, so that each subdivision had a similar number of data values (see Sect. II).

The data of each block was then run through SBOP, only leaving as variable the orbital period. The other parameters were set as fixed, using the updated orbital solution, as it is the best possible fit to the whole data set and these parameters should remain nearly constant over time. This way, the focus of the study was on the evolution of the $P_{\rm orb}$. As shown in Table II, the results obtained show that the variations detected between the B_1, B_2 and B_3 orbital periods are small, and they are compatible within 2σ-uncertainties. In Fig. 3 we show the results for the fitted orbital period of each subset as a function of time. No clear trend is seen in the figure.

C. Third analysis. Two blocks.

The following step taken in the study of the orbital period evolution was to divide the data set into two blocks, consisting of the data from 1998–2005 and 2007–2022. These blocks contain a similar number of data points (279 and 283, respectively), which allowed us to make variations to the parameters having subsets large enough for the results to be significant. These two subsets were the same ones used in the following analyses, as shown in Table II: C_1 and C_2, C_3 and C_4, C_5 and C_6.

The first study done on these two blocks was similar

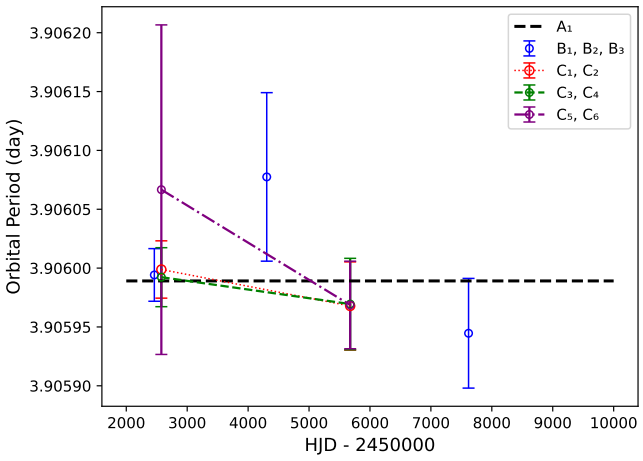

FIG. 3: Orbital periods and 1σ uncertainties fitted to each subset of data plotted as a function of time.

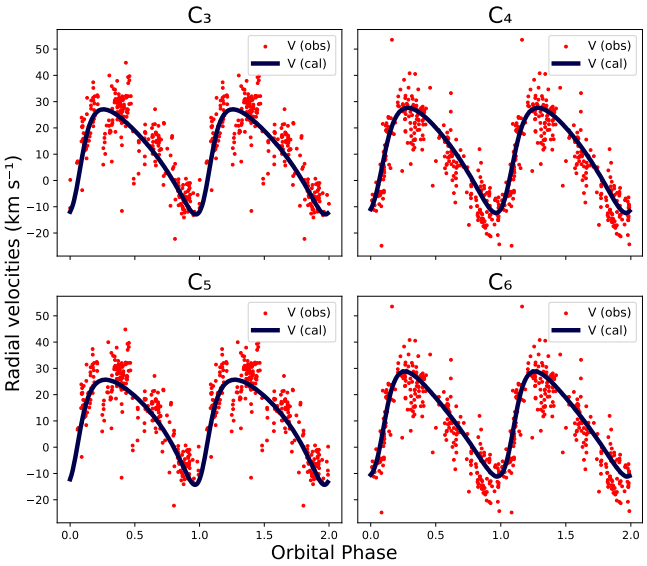

FIG. 4: Radial velocities plotted as a function of the orbital phase, for the subsets C_3 and C_4 (top) and C_5 and C_6 (bottom). Two cycles are shown for better display.

to the previous one reported in Subsect. IV B. The two subsets (C_1 and C_2) were run through SBOP leaving the orbital period as the only variable parameter. The orbital period was fitted to the two data subsets using the other parameters as fixed, and when compared we could see a very small decrease in the value of the orbital period (Table II), compatible within 1σ-uncertainties (Fig. 3).

Having two blocks with enough data values in each one enabled us to allow other parameters to be variable, and see how not fixing them affected the evolution of the orbital period. To do so, two more analyses were conducted. The first one involved setting as variable parameters both the orbital period $P_{\rm orb}$ and the eccentricity e. The obtained results are shown in Table II as C_3 and C_4. We could observe how the eccentricity varied by fitting it with smaller data sets and its difference between C_3 and C_4. The orbital period, however, did not vary much from previous results, obtaining similar values and uncertainties to the ones obtained in C_1 and C_2 (see Fig. 3).

The last analysis conducted involved the same two subsets of data (in this case the results are presented in Table II as C_5 and C_6), which were run through SBOP setting as variable the orbital period $P_{\rm orb}$, the epoch of periastron T_0, the eccentricity e and the argument of periastron ω. This allowed for greater variation and bigger uncertainties for the parameters when fitting the orbital solutions to the smaller subsets, but allowed us to see the effects of this variability on the evolution of the orbital period. However, the results obtained for C_5 and C_6 where similar to previous attempts, as only a slight decrease of $P_{\rm orb}$ was observed within 1σ-uncertainties (see Fig. 3). The other parameters had a greater variation but always within uncertainties, which were slightly larger than the ones obtained using the whole data set in A_1.

We show in Fig. 4 the radial velocities plotted as a function of time for the two subsets, alongside the fitted solution for both C_3, C_4 and C_5, C_6. The variation in the fitted solution curve for the subsets is due to the different output values for the eccentricity of each subset of data, because e was left variable in these analyses.

In addition to the aforementioned analyses, alternative approaches were explored but deemed irrelevant to this work. We performed certain analyses excluding the data points that exhibited high uncertainties. To achieve this, we divided the data set into subsets based on the observation epoch and the specific telescope employed. Then, the mean uncertainty was computed for each subset. Data points within a subset having an associated uncertainty that surpassed a threshold of three times the mean uncertainty for that subset were subsequently removed. It is worth noting that only a few number of data points were ultimately eliminated. After excluding measurements with substantial associated uncertainties, the data sets were processed with SBOP following the same methodology explained in Subsect. IV B. The results were compared with the ones obtained in Subsect. IV B, revealing no discernible discrepancies. This outcome can be attributed to the fact that only a few points where eliminated from the data set, suggesting that treating the data set following this procedure had no impact on the resulting outcomes, so this method was discarded.

V. ORBITAL PERIOD EVOLUTION DUE TO GW EMISSION

One of the physics phenomena that could lead to a decrease in the orbital period of the binary system LS 5039 is the energy loss due to the emission of gravitational waves (GWs). We assessed the impact that this process could have in our system by calculating the ratio of

period decrease (Peters & Matthews 1963, Weisberg & Taylor 2004), which according to general relativity (GR) is given by:

$$\dot{P}_{\rm orb}^{\rm GR} = -\frac{192\pi G^{\frac{5}{3}}}{5c^5}\left(\frac{P_{\rm orb}}{2\pi}\right)^{-\frac{5}{3}}\left(1+\frac{73}{24}e^2+\frac{37}{96}e^4\right)\times \left(1-e^2\right)^{-\frac{7}{2}} m_1 m_2 \left(m_1+m_2\right)^{-\frac{1}{3}} \tag{1}$$

The values inserted in Eq. 1 were $P_{\rm orb} = 3.90599$ day, $e = 0.35$, corresponding to the orbital period and the eccentricity values from the updated orbital solution for LS 5039, and $m_1 = 1.4$–2.5 $M_\odot$, $m_2 = 20$–25 $M_\odot$ which are the masses of the compact object and the companion star, respectively. We used the range of masses for both the compact object and the star (M. Ribó, priv. comm.) to determine the limits of the ratio of orbital period decrease. Inserting the values for $P_{\rm orb}$, e and the mass ranges into Eq. 1, we obtained the following results:

$$\begin{aligned} \dot{P}_{\rm orb,min}^{\rm GR} &= -0.5\times10^{-13}\ {\rm s/s} \\ \dot{P}_{\rm orb,max}^{\rm GR} &= -1.0\times10^{-13}\ {\rm s/s} \end{aligned} \tag{2}$$

Using these ratios, we can compute the orbital period variation that we would expect due to energy loss in the form of emission of GWs throughout the observation time interval. We used the values for the average time at which the data points were collected for the subsets C_3 and C_4, to determine the optimal time interval used to compute the orbital period variation. We obtained a time interval around 3099 days, and used the results from Eq. (2) to obtain the decrease of the orbital period that we would measure due to GWs emission:

$$\begin{aligned} \Delta P_{\rm orb,min} &= -1.3\times10^{-5}\ {\rm s} \\ \Delta P_{\rm orb,max} &= -2.7\times10^{-5}\ {\rm s} \end{aligned} \tag{3}$$

The computed decrease of the orbital period for the same time interval, using the results obtained in C_3 and C_4 is:

$$\Delta P_{\rm orb} = -3\pm6\ {\rm s} \tag{4}$$

Comparing the results from Eq. (3) and (4), it is shown how the decrease in the orbital period due to energy lost due to the emission of GWs is five orders of magnitude less than the differences and uncertainties we computed.

VI. CONCLUSIONS

In this work we present a study of the orbital parameters of the LS 5039 binary system. We have fitted new radial velocities of LS 5039 using the SBOP program and obtained a new orbital solution. In particular, we have found $P_{\rm orb} = 3.90599 \pm 0,00002$ day, a result an order of magnitude more precise than the previous orbital solution from Casares et al. (2005). The other obtained orbital parameters are $e = 0.35 \pm 0,03$, $\omega = 243 \pm 5°$, $v_0 = 10.5 \pm 0.3$ km s^{-1} and $K = 20.0 \pm 0.6$ km s^{-1}. With these new orbital parameters we have studied the evolution of the orbital period over time. We have divided the data into subsets following different criteria, analysing each subset using SBOP and comparing the obtained results for the orbital parameters, revealing no significant variation in the orbital period within the observed time frame. We have also computed the theoretical impact that the energy loss in the form of emission of gravitational waves could have on the evolution of the orbital period, concluding that it was too small to have a relevant influence over the results.

Acknowledgments

I would like to thank my advisor Dr. Marc Ribó for his patience and guidance, and the time dedicated to this work. I would also like to thank Dr. J. Casares for providing the data for this study. Finally, I want to thank my family and Èlia for their constant support.

[1] Aragona, C., et al. 2009, *The orbits of the γ-ray binaries LS I +61 303 and LS 5039*, ApJ, 698, 514
[2] Bordas, P. 2023, *Binary systems at gamma-rays*, PoS(Gamma2022)017
[3] Casares, J., et al. 2005, *A possible black hole in the γ-ray microquasar LS 5039*, MNRAS, 364, 899
[4] Casares, J., et al. 2012, *On the binary nature of the γ-ray sources AGL J2241+4454 (= MWC 656) and HESS J0632+057 (= MWC 148)*, MNRAS, 421, 1103
[5] Dubus, G. 2013, *Gamma-ray binaries and related systems*, A&A, 21, 64
[6] Etzel, P. 2004, SBOP: Spectroscopic Binary Orbit Program (San Diego State University)
[7] Hinton, J.A., & Hofmann, W. 2009, *Teraelectronvolt Astronomy*, ARA&A, 47, 523
[8] McSwain, M.V., et al. 2001, *The orbit of the massive X-ray binary LS 5039*, ApJ, 558, L43
[9] McSwain, M.V., et al. 2004, *The N enrichment and supernova ejection of the runaway microquasar LS 5039*, ApJ, 600, 927
[10] Paredes, J.M., & Bordas, P. 2019, *Phenomenology of gamma-ray emitting binaries*, RLSFN, 30, 107
[11] Peters, P.C., & Mathews, J. 1963, *Gravitational Radiation from Point Masses in a Keplerian Orbit*, Phys. Rev., 131, 435
[12] Weisberg, J., & Taylor, J. 2004, *Relativistic Binary Pulsar B1913+16: Thirty Years of Observations and Analysis*, ASPC, 328, 25